Available online at www.elixirpublishers.com (Elixir International Journal)

Computational Chemistry

Elixir Comp. Chem. 89 (2015) 36730-36741

ISSN: 2229-712X

Electronic Structure Investigations of 3 and 5- Diamino-1,2,4-Triazole By UV–Visible , NMR Spectral Studies and Homo-Lumo Analysis by *AB Initio* and DFT Calculations

D.Cecily Mary Glory[1], R.Madivanane[2] and K.Sambathkumar[3*]

[1] Research scholar R& D centre, Bharathar University.

[2]Department of physics, Mahatma Government College, Maye, Puducherry,India.

[3]Department of Physics, A.A. Government Arts College, Villupuram-605602.

ARTICLE INFO

Article history:

Received: 28 October 2015;

Received in revised form:

25 November 2015;

Accepted: 02 December 2015;

Keywords

FTIR,

FT-Raman,

HOMO- LUMO,

NMR,

UV,

DAT.

ABSTRACT

Quantum chemical calculations of energies, geometrical structures and electronic absorption spectra of 3,5-diamino-1,2,4-triazole (DAT) were carried out by ab initio HF/6-311+G(d,p), DFT (B3LYP/6-311+G(d,p)). The optimized geometric bond lengths and bond angles obtained by HF method show best agreement with the experimental values. Comparison of the observed fundamental vibrational frequencies of DAT with calculated results by HF and density functional methods indicates that B3LYP is superior to the scaled Hartree-Fock approach for molecular vibrational problems. The difference between the observed and scaled wave number values of most of the fundamentals is very small. A detailed interpretation of the FT-IR and FT- Raman, NMR spectra of DAT was also reported. Thermodynamic properties were also calculated and discussed. UV–vis spectrum of the compound was recorded and the electronic properties, such as HOMO and LUMO energies, were performed by time dependent density functional theory (TD-DFT) approach. Finally the calculations results were applied to simulated infrared and Raman spectra of the title compound which show good agreement with observed spectra. The Mulliken charge analysis indicates that the nitrogen atoms of the triazole ring and the amino group attached to the ring are the main reactive centers of 3,5-diamino-1,2,4-triazole. And the temperature dependence of the thermodynamic properties of constant pressure (Cp), entropy (S) and enthalpy change (ΔH0→T) for DAT were also determined.

Introduction

A good number of five membered aromatic systems having three heteroatoms at symmetrical positions have been studied because of their interesting physiological properties. The presence of three nitrogens in triazole provides an interesting class of compounds. 3-Amino-1,2,4-triazole (Amitrole) has extensive biological activity, including antibacterial and herbicidal action via effects on DNA and related molecules; it inhibits the action of catalase and lactoflavin synthesis, and the formation of chlorophyll in plants [1–5]. Antiviral properties have been found for some derivatives of 5-amino-1,2,4-triazole ribofuranoside (e.g. Ribavirin) [6], and the closely related 5-amino-imidazole-4-carboxamide riboside (e.g. Aicar) [7]. A number of crystallographic studies, discussed below, have been reported for other aminotriazoles, arising from interest in their diverse biological activity. Although triazole and its derivatives show a wide spectrum of activity, literature search revealed that not much has been reported about the structure/activity relationship of this class of compounds. The electronic properties in particular the HOMO-LUMO gap of a compound gives information about the stability and chemical reactivity of the compound [10]. In order to gain an insight into the relationship between structure and reactivity, a derivative of triazole (3,5-diamino- 1,2,4-triazole), a molecule with two symmetrical positioned NH2 groups has been chosen for this study. The vibrational frequencies of parent triazole compound have been reported [11, 12] based on classical or low level quantum chemical calculations. Kumar et.al., [12] also reported on the influence of hydrogen bonding on the vibrational spectroscopic properties of triazole and 3,5-diamino-1,2,4-triazole using DFT at B3LYP/6-31+G(d,p) level of theory. Therefore using classical ab *initio* methods based on selfconsistent field molecular orbital Hartree-Fock theory (HF), density functional theory (DFT) and time dependent density functional theory (TD-DFT) with the 6-31+G(d,p) basis set, we investigate the optimized structure, Mulliken charge distributions, NMR, thermodynamic and electronic transition of 3,5-diamino-1,2,4-triazole. The electronic absorption spectra obtained theoretically have been compared with the experimental absorption bands.

Experimentation

The pure compound 3,5-diamino-1,2,4-triazole was purchased from Lancaster chemical company, U.K. and used as such without any further purification. The room temperature Fourier transform infrared (FTIR) spectrum of

Tele: 09994188861

E-mail addresses: sa75kumar@yahoo.co.in

DAT is recorded in the range of 4000 - 400 cm^{-1} at a resolution of ± 1 cm^{-1} using a BRUKER IFS 66V FTIR spectrophotometer equipped with a cooled MCT detector. Boxcar apodization is used for the 250 averaged interferograms collected for both the samples and background. The FT-Raman spectrum is recorded on a computer interfaced BRUKER IFS model interferometer, equipped with FRA 106 FT-Raman accessories in the 3500 - 50 cm^{-1} Stokes region, using the 1064 nm line of Nd:YAG laser for excitation operating at 200 mW power. The reported wave numbers are believed to be accurate within ± 1 cm^{-1}.The UV-visible absorption spectra of DAT are examined in the range 200 - 600 nm using SHIMADZU UV-1650 PC, UV-VIS recording spectrometer. The UV pattern is taken from 10^{-5} molar solution of DAT, solved in DMSO.

Computational Methodology

Density functional theory calculations are carried out for DAT, Hartree-Fock (HF) and DFT calculations using GAUSSIAN 09W program package [13]. The geometry optimization was carried out using the initial geometry generated from the standard geometrical parameters is minimized without any constraint on the potential energy surface at Hartree-Fock level adopting the standard 6-311+G(d,p) basis set. This geometry is then re-optimized again at DFT level employing the B3LYP keyword, which invokes Becke's three-parameter hybrid method [14] using the correlation function of Lee *et al*. [15], implemented with the same basis set for better description of the bonding properties of amino group. All the parameters are allowed to relax and all the calculations converged to an optimized geometry which corresponds to a true minimum, as revealed by the lack of imaginary values in the wave number calculations. The multiple scaling of the force constants are performed according to SQM procedure [16] using selective scaling in the natural internal coordinate representation [17]. Transformation of force field, the subsequent normal coordinate analysis including the least square refinement of the scale factors and calculation of the total energy distribution (TED) are done on a PC with the MOLVIB program (version V7.0 - G77) written by Sundius [18,19]. The systematic comparison of the results from DFT theory with results of experiments has shown that the method using B3LYP functional is the most promising in providing correct vibrational wave numbers. The calculated geometrical parameters are compared with X-ray diffraction result [20]. Normal coordinate analyses were carried out for DAT to provide a complete assignment of fundamental frequencies. For this purpose, the full set of 36 standard internal coordinates (containing 6 redundancies) for DAT is defined as given in Table 1. From these, a non-redundant set of local symmetry coordinates were constructed by suitable linear combinations of internal coordinates following the recommendations of Fogarasi *et al*. [17] and that is summarized in Table 2. The theoretically calculated force fields are transformed to this set of vibrational coordinates and used in all subsequent calculations.

Prediction of Raman intensities

The Raman activities (S_i) calculated with the GAUSSIAN 09W program are subsequently converted to relative Raman intensities (I_i) using the following relationship derived from the basic theory of Raman scattering [21-23]

$$I_i = \frac{f(\nu_0 - \nu_i)^4 Si}{\nu_i \left[1 - \exp\frac{-hc\nu_i}{kT}\right]} \quad \ldots (1)$$

where ν_0 is the exciting frequency in cm^{-1}, ν_i the vibrational wave number of the i^{th} normal mode, h, c and k are the fundamental constants and *f* is a suitably chosen common normalization factor for all the peak intensities.

Table 1. Definition of internal coordinates of 3,5-diamino-1,2,4-triazole

No.(i)	Symbol	Type	Definition [a]
Stretching			
1	ri	N-H	N4-H12
2	Ri	N-N	N1-N2
3-8	qi	C-N	C3-N2, C3-N4, C3-N9, C5-N4, C5-N1, C5-N6
9-12	Pi	N-H_2	N6-H7,N6-H8,N9-H10,N9-H11
In-plane bending			
13-17	αi	Ring	N1-N2-C3,N2-C3-N4,C3-N4-C5,N4-C5-N1, C5-N1-N2
18,19	βi	C-N-H	C5-N4-H12,C3-N4-H12
20-23	νi	H-N-C	H7-N6-C5,H8-N6-C5,H11-N9-C3,H10-N9-C3
24-27	σi	N-C-N	N6-C5-N4,N6-C5-N1,N9-C3-N4,N9-C3-N2
Out-of-plane bending			
28	ψi	N-H	H12-N4-C5-C3
29,30	μi	N-C	N6-C5-N4-N1,N9-C3-N4-N2
Torsion			
31-34	τi	t Ring	N1-N2-C3-N4,N2-C3-N4-C5,C3-N4-C5-N1,N4-C5-N1-N2
35,36	τi	t C-NH2	C3-N9-H11-H10,C5-N6-H7-H8

[a]For numbering of atoms refer Fig.1

Table 2. Definition of local symmetry coordinates of 3,5-diamino-1,2,4-triazole

No. (i)	Type	Definition
1	N H	r_1
2	NN	R_2
3-8	CN	q_3,q_4,q_5,q_6,q_7,q_8
9,10	NH_2 ss	$(P_9 + P_{10}) / \sqrt{2}$,$(P_{11} + P_{12}) / \sqrt{2}$
11,12	NH_2 ass	$(P_9 - P_{10}) / \sqrt{2}$,$(P_{11} - P_{12}) / \sqrt{2}$
13	Rbend1	α_{13} +a(α_{14} + α_{15})+b(α_{16} + α_{17})
14	Rbend2	(a-b)(α_{14} + α_{15})+(1-a)(α_{16} + α_{17})
15	bNH	$(\beta_{18} - \beta_{19})/\sqrt{2}$
16,17	NH_2 rock	$(\nu_{20} - \nu_{21})/\sqrt{2}$, $(\nu_{22} - \nu_{23})/\sqrt{2}$
18,19	NH_2 twist	$(\nu_{20} + \nu_{21}) / \sqrt{2}$,$(\nu_{22} - \nu_{23})/\sqrt{2}$
20,21	NH_2 sciss	$(\nu_{20} - \nu_{21}) / \sqrt{6}$,$(\nu_{22} - \nu_{23})/\sqrt{6}$
22,23	bCN	$(\sigma_{24} - \sigma_{25})/\sqrt{2}$ $(\sigma_{26} - \sigma_{27})/\sqrt{2}$
24	ω N H	ψ_{28}
25,26	ω NC	μ_{29} , μ_{30}
27	Torsion1	τ_{31} +b(τ_{32}+τ_{33})+a(τ_{34}+τ_{35})
28	Torsion2	(a-b)(τ_{35}- τ_{34})+(1-a)(τ_{33}-τ_{32})
29,30	t C-NH_2 wag	τ_{36} ,τ_{37}

[a] The internal coordinates used here are defined in Table 1.

Table 3. Optimized geometrical parameters of 3,5-diamino-1,2,4-triazole obtained by HF/6-31G+(d,p) and B3LYP/6-31+G(d,p) density functional theory calculations

	Value (Å)			Value (°)				Value (°)		
Bond lengths (Å)	**HF/ 6-1G+(d,p)**	**B3LYP/ 6-31G+(d,p)**	**Exp[20]**	**Bond angles(Å)**	**HF/ 6-31G+(d,p)**	**B3LYP/ 6-1G+(d,p)**	**Exp[20]**	**Dihedral angle**	**HF/ 6-31G+(d,p)**	**B3LYP/ 6-31G+(d,p)**
N1-N2	1.4080	1.4394	1.369	N2-N1-C5	101.863	106.881	124.7	C5-N1-N2-C3	0.0326	2.4058
N1-C5	1.3142	1.3211	1.334	N1-N2-C3	109.752	106.881	125.6	N2-N1-C5-N4	-180.0716	-1.9461
N2-C3	1.3327	1.3210		N2-C3-N4	120.618	110.523		N2-N1-C5-N6	-180.0112	-1.9517
C3-N4	0.9856	1.3899	1.360	N4-C3-N9	129.629	126.255	118.0	N1-N2-C3-N4	-0.0325	174.433
C3-N9	1.3326	1.3816	1.386	C3-N4-C5	109.792	123.118		N1-N2-C3-N9	-180.0088	0.8058
N4-C5	1.3426	1.3899	1.335	C3-N4-H12	125.296	105.135	123.3	N2-C3-N4-C5	180.0839	-179.2584
N4-H12	1.3713	1.0034		C5-N4-H12	124.910	127.422		N2-C3-N4-H12	0.1076	-175.7134
C5-N6	1.3516	1.3817	1.470	N1-C5-N4	103.910	127.441	122.9	N9-C3-N4-C5	0.0177	4.2224
N6-H7	0.9868	1.0067		N1-C5-N6	114.681	110.523		N9-C3-N4-H12	179.9941	134.9789
N6-H8	0.9872	1.0062		N4-C5-N6	124.031	126.253	123.7	N2-C3-N9-H10	180.0049	-8.5324
N9-H10	0.9879	1.0066		C5-N6-H7	121.287	123.119		N2-C3-N9-H11	-0.08	-49.0645
N9-H11	0.9880	1.0063		C5-N6-H8	119.841	119.545	109.0	N4-C3-N9-H10	0.0322	167.4242
				H7-N6-H8	120.793	114.732	122.6	N4-C3-N9-H11	-180.0528	0.7971
				C3-N9-H10	119.365	115.337	128.7	C3-N4-C5-N1	0.0042	-175.7102
				C3-N9-H11	119.014	119.589		C3-N4-C5-N6	-180.0065	-179.7102
				H10-N9-H11	122.296	114.753	155.5	H12-N4-C5-N1	-180.0221	-179.1387
								H12-N4-C5-N6	-0.057	4.354
								N1-C5-N6-H7	0.1762	135.0288
								N1-C5-N6-H8	0.0052	-8.3593
								N4-C5-N6-H7	-180.0451	-49.0283
								N4-C5-N6-H8	0.0339	167.5836

For numbering of atoms refer Fig. 1
Ref.no.[20]

Results and Discussion

Molecular geometry

The optimized molecular structure of DAT along with numbering of atoms is shown in Fig. 1.

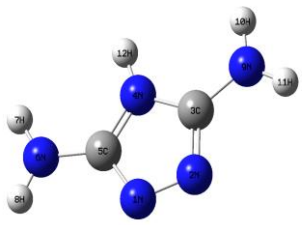

Fig 1. Molecular structure of 3,5-diamino-1,2,4-triazole

The optimized structure parameters of DAT obtained by DFT-B3LYP/6-311+G(d,p) and HF/6-311+G(d,p) levels are listed in Table 3. From the structural data given in Table 3, it is observed that the various bond lengths are found to be almost same at HF/6-311+G(d,p) level of theory, in general slightly overestimates bond lengths but it yields bond angles in excellent agreement with the HF and B3LYP methods. The calculated geometric parameters can be used as foundation to calculate the other parameters for the compound. The optimized molecular structure of DAT reveals that the heterocyclic rings of amino group are in planar. Inclusion of NH atoms known for its strong electron-withdrawing nature, in heterocyclic position, is expected to increase a contribution of the resonance structure, in which the electronic charge is concentrated at this site. This is the reason for the shortening of bond lengths N6-H7 = 0.9868, N6-H8 = 0.9872, N9-H10 = 0.9879 Å and N9-H11 = 0.988 Å obtained by HF method. The same bond lengths calculated by DFT method is found to be 1.0062 Å and 1.067 Å. In DAT, the N-H bond lengths are 1.3713 Å for HF method and 1.0034 B3LYP methods. The ring carbon atoms in substituted N-heterocyclic exert a larger attraction on the valence electron cloud of the nitrogen atom resulting in an increase in the N-N force constants and a increasing in the corresponding bond length. It is evident from the N-C bond lengths ranging from 0.9856 Å to 1.3426 Å by HF method and from 1.3210 to 1.3899 by B3LYP method in the N-heterocyclic rings of DAT, whereas the N-N bond lengths in DAT for 1.4080 Å and for 1.4394 Å by HF and B3LYP methods, respectively. The heterocyclic rings appear to be a little distorted because of the NH_2 group substitution as seen from the bond angles N2-C3-N4 which are calculated as 120.618° and 110.523° respectively, by HF and B3LYP methods and they are smaller than typical hexagonal angle of 120°. From the theoretical values, it is found that most of the optimized bond lengths are slightly larger than the experimental values, due to that the theoretical calculations belong to isolated molecules in solid state. Comparing bond angles and lengths of B3LYP with those of HF, as a whole the formers are bigger than the later and the B3LYP calculated values correlate well compared with the experimental data.

And several thermodynamic properties like heat capacity, zero point energy, entropy along with the global minimum energy of 3,5-diamino-1,2,4-triazole have been obtained by ab initio HF and density functional methods using 6-311+G(d,p) basis set and the calculations are presented in Table 4.

Table 4. The thermodynamic parameters of 3,5-diamino-1,2,4-triazole along with the global minimum energy calculated at HF/6-31+G(d,p) and B3LYP /6-31+G(d,p) methods.

Parameters	HF/ 6-311++G(d,p)	B3LYP/ 6-311++G(d,p)
Optimized global minimum Energy,(Hartrees)	-350.8159	-352.9186
Total energy(thermal), E_{total} (kcal mol^{-1})	66.624	62.146
Translational	0.889	0.889
Rotational	0.889	0.889
Vibrational	64.846	60.369
Molar capacity at constant volume,(cal mol^{-1} k^{-1}),Total	23.457	24.805
Translational	2.981	2.981
Rotational	2.981	2.981
Vibrational	17.496	18.843
Entropy Total	77.394	79.277
Translational	39.690	39.680
Rotational	26.829	26.917
Vibrational	10.875	12.649
Zero point vibrational energy, (Kcal mol^{-1})	62.6920	57.9578
Rotational constants (GHZ)		
A	7.4860	7.4968
B	2.2170	2.1003
C	1.7104	0.0791
Rotational temperature (Kelvin)		
	0.3592	0.3597
	0.1064	0.1008
	0.0820	0.0791

The difference in the values calculated by both the methods is only marginal. Scale factors have been recommended for an accurate prediction in determining the zero-point vibration energy (ZPVE), and the entropy (Svib). The variation in the ZPVE seems to be insignificant. The total energy and the change in the total entropy of 3,5-diamino-1,2,4-triazole at room temperature at B3LYP/6-311+G(d,p) and HF/6-311+G(d,p) level of theory are only marginal.

Non-Linear Optical (NLO) Properties

The potential application of the title compound in the field of nonlinear optics demands, the investigation of its structural and bonding features contribution to the hyperpolarizability enhancement, by analysing the vibrational modes using IR and Raman spectroscopy. Many organic molecules, containing conjugated π electrons are characterized by large values of molecular first hyperpolarizabilities, are analysed by means of vibration spectroscopy [24]. In most of the cases, even in the absence of inversion symmetry, the strongest band in the IR spectrum is weak in the Raman spectrum and vice-versa. But the intramolecular charge from the donor to acceptor group through a π-bond conjugated path can induce large variations of both the molecular dipole moment and the molecular polarizability, making IR and Raman activity strong at the same time. The experimental spectroscopic behavior described above is well accounted for a calculations in π conjugated systems that predict exceptionally infrared intensities for the same normal modes. The first hyperpolarizability (*β*) of this novel molecular system is calculated using the *ab initio* quantum mechanical method, based on the finite-field approach. In the presence of an applied electric field, the energy of a system is a function of the electric field. The first hyperpolarizability is a third-rank tensor that can be described by a 3x3x3 matrix. The 27 components of the 3D matrix can be reduced to 10 components due to the Kleinman symmetry [25]. The components of β are defined as the coefficients in the Taylor series expansion of the energy in the external electric field. When the electrical field is weak and homogeneous, this expansion becomes

$$E = E_0 - \sum_i \mu_i F^i - \frac{1}{2}\sum_{ij} \alpha_{ij} F^i F^j - \frac{1}{6}\sum_{ijk} \beta_{ijk} F^i F^j F^k - \frac{1}{24}\sum_{ijkl} \nu_{ijkl} F^i F^j F^k F^l \quad \ldots (2)$$

where E_0 is the energy of the unperturbed molecules, F_α is the field at the origin and μ_α, $\alpha_{\alpha\beta}$ and $\beta_\alpha\beta_\gamma$ are the components of dipole moment, polarizability and the first hyperpolarizabilities, respectively. The total static dipole moment μ, the mean polarizability α_0 and the mean first hyperpolarizability β_0, using the x, y, z components they are defined as:

$\mu = (\mu_x^2+\mu_y^2+\mu_z^2)^{1/2}$

$\alpha_0 = (\alpha_{xx} + \alpha_{yy} + \alpha_{zz})/3$

$\alpha = 2^{-1/2} [(\alpha_{xx} - \alpha_{yy})^2 + (\alpha_{yy} - \alpha_{zz})^2 + (\alpha_{zz} - \alpha_{xx})^2 + 6\alpha_{xx}^2)^{1/2}$

$\beta_0 = (\beta_x^2+\beta_y^2+\beta_z^2)^{1/2}$

$\beta_{vec} = 3/5[(\beta_x^2+\beta_y^2+\beta_z^2)^{1/2}]$

Where

$\beta_x = \beta_{xxx} + \beta_{xyy} +\beta_{xzz}$

$\beta_y = \beta_{yyy} + \beta_{yxx} +\beta_{yzz}$

$\beta_z = \beta_{zzz} + \beta_{zxx} +\beta_{zyy}$

The β_0 components of GAUSSIAN 09W output are reported in atomic units and therefore the calculated values are converted into e.s.u. units (1 a.u. = 8.3693×10^{-33} e.s.u.). The calculated value of hyperpolarizability and polarizability of DAT are tabulated in Table 5.

Table 5. Nonlinear optical properties of 3,5-diamino-1,2,4-triazole calculated at HF/6-311++G(d,p) with B3LYP/6-311+G(d,p) method and basis set

NLO behaviour	HF/ 6-311+G(d,p)	B3LYP/ 6-311+G(d,p)
Dipole moment(μ)	2.3672Debye	2.3502Debye
Mean polarizability (α)	0.4695x 10^{-30} esu	1.3337x10^{-30} esu
Anisotropy of the polarizabilty (Δα)	1.4071x10^{-30} esu	1.0317x10^{-30} esu
First hyperpolarizability (β)	0.9134x 10^{-30} esu	0.8890 x10^{-30} esu
Vector – first hyperpolarizability (βvec)	0.5480x10^{-30} esu	0.5333 x10^{-30} esu

The title molecule (DAT) is an attractive object for future studies of non-linear optical properties.

NMR spectral analysis

The molecular structure of DAT is optimized by using B3LYP method with 6-311+G basis set. Then, GIAO ^{13}C calculations of the title compound are calculated and compared with experimental values [26] are shown in Table 6. Relative chemical shifts were then estimated by using the corresponding TMS shielding calculated in advance at the theoretical level as reference. Changes in energy needed to flip protons are called chemical shifts. The location of chemical shifts (peaks) on a NMR spectrum are measured from a reference point that the hydrogens in a standard reference compound – $(CH3)_4Si$ or tetramethylsilane (TMS) – produce.

Table 6. Theoretical chemical shifts (^{13}C, ^{1}H) of 3,5-diamino-1,2,4-triazole by B3LYP/6-311+G(d,p) method (ppm)].

Atom position	B3LYP		Expt
	Isotropic chemical shielding tensor(σ)(ppm)	6-311+G(d,p)	
N1	-115.9860	-115.986	
N2	60.0226	60.0226	
C3	5.2941	177.171	
N4	-75.8897	-75.889	
C5	-19.2508	201.716	
N6	204.1746	204.175	
H7	30.2668	1.6153	2.60
H8	29.8889	1.9972	2.60
N9	187.1121	187.112	
H10	29.1160	2.7661	2.62
H11	30.5743	1.307	2.62
H12	24.6643	7.218	7.55

[a] Taken from Ref [39] and $\Delta(\delta_{exp}-\delta_{the})$; difference between respective chemical shifts.

The amount of energy necessary to flip protons in TMS is assigned the arbitrary value of zero δ. Chemical shifts are measured in parts permillion magnetic field strength difference (δ-scale), relative to TMS. All the calculations were performed using Gauss view molecular visualization program and Gaussian 09W program package. The result shows that the range ^{13}C NMR chemical shift of the typical organic compound usually is >100 ppm [27,28], the accuracy ensures reliable interpretation of spectroscopic parameters. It is true from the above literature value in our present study, that the title compound also shows the same. In practice, it is easier to fix the radio wave frequency and vary the applied magnetic field than it is to vary the radio wave frequency. The magnetic field "felt" by a hydrogen atom is composed of both applied and induced fields. The induced field is a field created by the electrons in the bond to the hydrogen and the electrons in nearby π bonds. When the two fields reinforce each other, a smaller applied field is required to flip the proton. In this situation, a proton is said to be deshielded. When the applied and induced fields oppose each other, a stronger field must be applied to flip the proton. In this state, the proton is shielded. Electronegative atoms such as Br, O2, NH2 and halogens deshield hydrogens. The extent of deshielding is proportional to the electronegativity of the heteroatom and its proximity to the hydrogen. Electrons on a heterocyclic ring, double bonded atoms, and triple bonded atoms deshield attached hydrogens. These bromine, amino and oxygen atoms show electronegative property, so that the chemical shift of C_3 and C_5 seems to be 177.171 and 201.716 ppm for DAT. The chemical shift of C_5 is greater than the other carbon values. This increase in chemical shift is due to the substitution of more electronegative amino atoms in the heterocyclic ring. The presence of electronegative atom attracts all electron clouds of carbon atoms towards the amino atoms, which leads to deshielding of carbon atom and net result in increase in chemical shift value. The NMR shielding surfaces of C_3 and C_5 is shown in this work the chemical shift (δ) for carbon atoms presented in the DAT has been studied and theoretical ^{13}C, ^{1}H-NMR isotropic shielding of carbon and Hydrogen atom are shown. In the NMR shielding surfaces, the blue region represents shielding and red region represents de-shielding are shown in Fig 2.

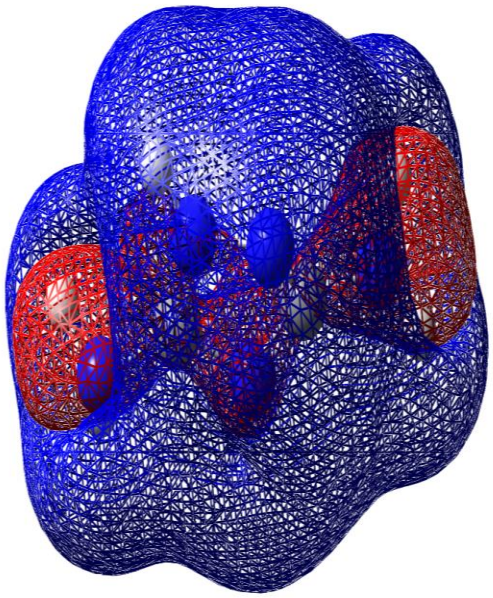

Fig 2. NMR shielding surface of 3,5-diamino-1,2,4-triazole

Frontier Orbital Energy

Many organic molecules that contain conjugated π electrons are characterized hyperpolarizabilities and are analyzed by means of vibrational spectroscopy. In most cases, even in the absence of inversion symmetry, the weakest bands in the Raman spectrum are strongest in the IR spectrum and vice versa. But the intra molecular charge transfer from the donor to accepter group through a single–double bond conjugated path can induce large variations of both the molecular dipole moment and the molecular polarizability, making IR and Raman activity strong at the same time. It is also observed in the title compound the bands in FTIR spectrum have their counterparts in Raman shows that the relative intensities in IR and Raman spectra are comparable resulting from the electron cloud movement through π conjugated frame work from electron donor to electron acceptor groups. Highest occupied molecular orbital (HOMO) and lowest unoccupied molecular orbital (LUMO) are very important parameters for quantum chemistry. Can determine the way the molecule interacts with other species; hence, they are called the frontier orbitals. HOMO, which can be thought the outermost orbital containing electrons, tends to give these electrons such as an electron donor. On the other hand; LUMO can be thought the innermost orbital containing free places to accept electrons [29]. Owing to the interaction between HOMO and LUMO orbital of a structure, transition state transition of π* type is observed with regard to the molecular orbital theory. The calculated self-consistent field (SCF) energy of DAT is -352.9186 a.u. Therefore, while the energy of the HOMO is directly related to the ionization potential, LUMO energy is directly related to the electron affinity. Energy difference between HOMO and LUMO orbitals is called as energy gap that is an important stability for structures. In addition, the pictorial scheme of few MOs of DAT is shown in Fig. 3.

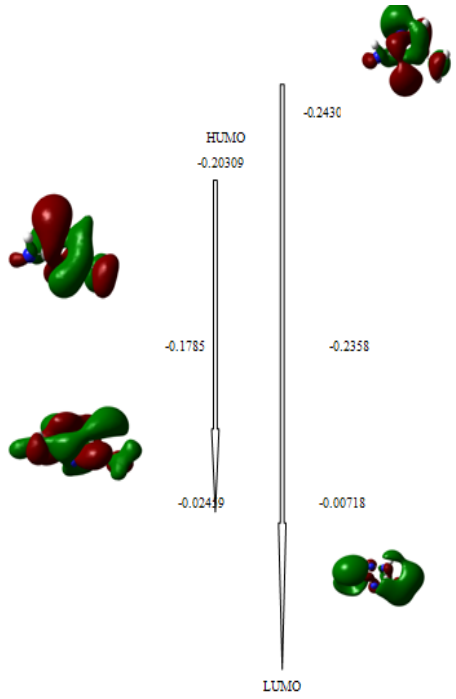

Fig 3. HOMO-LUMO plot of 3,5-diamino-1,2,4-triazole

HOMO is localized on the central ring and has partially contribution from the substitution groups such as oxygen and amino group. LUMO is quite localized on the central ring and has strong contribution from the substituted electronegative oxygen and amino group. The energy gap between HOMO and LUMO is -0.1785 a.u., which shows that charge transfer may be taking place from the ring to oxygen atom. As seen from the Fig. 3, HOMO-1 is very similar to HOMO, rotated by 90°.

Global and local reactivity descriptors

Based on density functional descriptors global chemical reactivity descriptors of molecules such as hardness, chemical potential, softness, electronegativity and electrophilicity index as well as local reactivity have been defined [30-33]. Pauling introduced the concept of electronegativity as the power of an atom in a molecule to attract electrons to it. Hardness (η), chemical potential (μ) and electronegativity (χ) and softness are defined as

$\eta = \frac{1}{2}(\partial 2E/\partial N2)V(r) = \frac{1}{2}(\partial \mu/\partial N)V(r)$

$\mu = (\partial E/\partial N)V(r)$

$\chi = -\mu = -(\partial E/\partial N)V(r)$

where E and V(r) are electronic energy and external potential of an N-electron system respectively. Softness is a property of molecule that measures the extent of chemical reactivity. It is the reciprocal of hardness.

$S = 1/\eta$

Using Koopman's theorem for closed-shell molecules, η, μ and χ can be defined as

$\eta = (I - A)/2$

$\mu = -(I + A)/2$

$\chi = (I + A)/2$

where A and I are the ionization potential and electron affinity of the molecules respectively. The ionization energy and electron affinity can be expressed through HOMO and LUMO orbital energies as $I = -E_{HOMO}$ and $A = -E_{LUMO}$. Electron affinity refers to the capability of a ligand to accept precisely one electron from a donor. However in many kinds of bonding viz. covalent hydrogen bonding, partial charge transfer takes places. Recently Parr *et al.* [30] have defined a new descriptor to quantify the global electrophilic power of the molecule as electrophilicity index (ω), which defines a quantitative classification of the global electrophilic nature of a molecule have proposed electrophilicity index (ω) as a measure of energy lowering due to maximal electron flow between donor and acceptor. They defined electrophilicity index (ω) as

$\omega = \mu^2/2\eta$

The usefulness of this new reactivity quantity has been recently demonstrated in understanding the toxicity of various pollutants in terms of their reactivity and site selectivity [34-36]. The calculated value of electrophilicity index describes the biological activity of DAT. All the calculated values of hardness, potential, softness and electrophilicity index are shown in Table 7.

Table 7. HOMO - LUMO energy gap and related molecular properties of 3,5-diamino-1,2,4-triazole

Molecular Properties	B3LYP/6-311+G(d,p)
HOMO	-0.2030
LUMO	-0.0245
Energy gap	-0.1785
Ionisation Potential (I)	0.2030
Electron affinity(A)	0.0245
Global softness(s)	11.2044
Global Hardness (η)	0.08925
Chemical potential (μ)	-0.11384
Global Electrophilicity (ω)	0.0725

UV-VIS spectral analysis

Ultraviolet spectra analysis of DAT have been investigated by TD-DFT/B3LYP/6-311+G (d,p) method in DMSO. The experimental absorption wavelengths (energies) and computed electronic values, such as absorption wavelengths (λ), excitation energies (EE), oscillator strengths (*f*), major contributions of the transitions and assignments of electronic transitions are shown in Table 8.

The absorption wavelengths are observed at 208.20 nm. Calculations of molecular orbital geometry show that the visible absorption maxima of this molecule correspond to the electron transition between frontier orbitals such as translation from HOMO to LUMO. As seen from the UV–VIS spectra calculated maxima values have been found to be 390.35,254.42 and 240.91 nm. The λ_{max} is a function of substitution, the stronger the donor character of the substitution, the more electrons pushed into the molecule, the larger the λ_{max}. These values may be slightly shifted by solvent effects. The role of substituent and of the solvent influences on the UV spectrum. This band may be due to electronic transition with in the ring through bridge (transition of π-π*). The calculated results involving the vertical excitation energies, oscillator strength (*f*) and wavelength are carried out and compared with measured experimental wavelength. TD-DFT/B3LYP/6-311+G(d,p) predict one intense electronic transition at eV (208.20 nm) with an oscillator strength *f* = 0.1461, in good agreement with the measured experimental data (λ_{exp} = 208.20 nm) as shown in Fig. 4.

Temperature dependence of Thermodynamic properties

The temperature dependence of the thermodynamic properties heat capacity at constant pressure (Cp), entropy (S) and enthalpy change (ΔH0→T) for DAT were also determined by B3LYP/6–311+G(d,p) method and listed in Table 9. The Figs 5-7 depicts the correlation of entropy (S), heat capacity at constant pressure (Cp) and enthalpy change (ΔH0→T) with temperature along with the correlation equations.

Table 8. The computed excitation energies, oscillator strength, electronic transition configuration wavelength of 3,5-diamino-1,2,4-triazole using TD-DFT/B3LYP/6-311+G(d,p).

	Experimental		Calculated				
Excited state	**λ (nm)**	**EE(eV)**	**EE(eV)**	**Oscillator strength *f***	**Configuration**	**CI expansion coefficient**	**λ (nm)**
1		5.007	3.1762	0.0000	26→30	-0.10486	390.35
					26→31	0.10420	
					26→32	0.17325	
2		5.397	4.8732	0.0000	25→33	0.14027	254.42
					25→34	-0.17590	
					25→39	0.10010	
					26→36	-0.110399	
3	208.20	5.9575	5.1464	0.1461	26→27	-0.13402	240.91
					26→30	0.17403	
					26→31	-0.14292	
					26→32	0.47218	
					26→33	-0.32918	

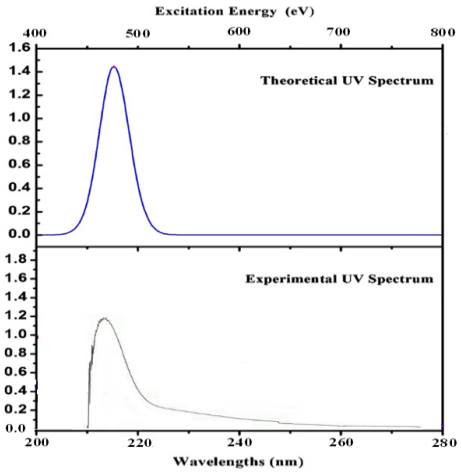

Fig 4. UV spectrum of 3,5-diamino-1,2,4-triazole.

From Table 9, one can find that the entropies, heat capacities, and enthalpy changes are increasing with temperature ranging from 100 to 1000 K due to the fact that the molecular vibrational intensities increase with temperature [37]. These observed relations of the thermodynamic functions vs. temperatures were fitted by quadratic formulas, and the corresponding fitting regression factors (R2) are all not less than 0.9995. The corresponding fitting equations for APH are

$S = 235.47 + 0.3\ T - 10.608 \times 10^{-4}\ T^2$

$Cp = 56.242 + 0.177\ T - 13.715 \times 10^{-4}\ T^2$

$\Delta H = -24.982 + 0.160\ T + 6.839 \times 10^{-4}\ T^2$

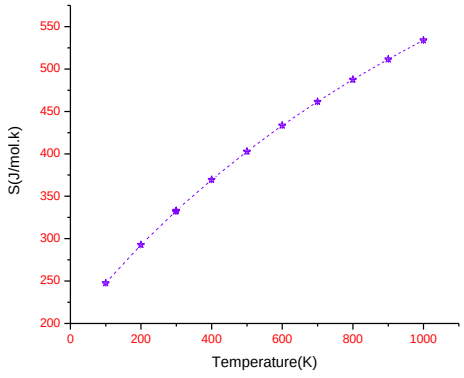

Fig 5.The effect of temperature on entropy (S) of 3,5-diamino-1,2,4-triazole

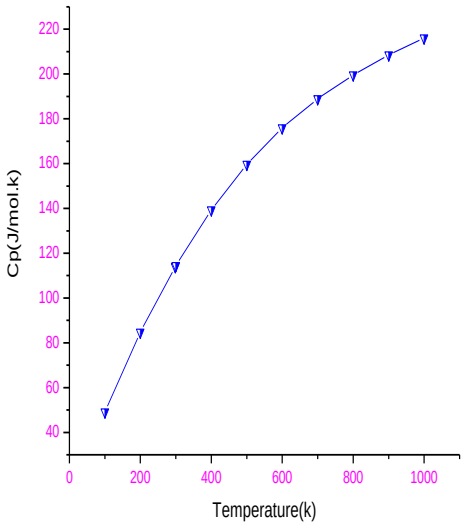

Fig 6. The effect of temperature on heat capacity (Cp) of 3,5-diamino-1,2,4-triazole

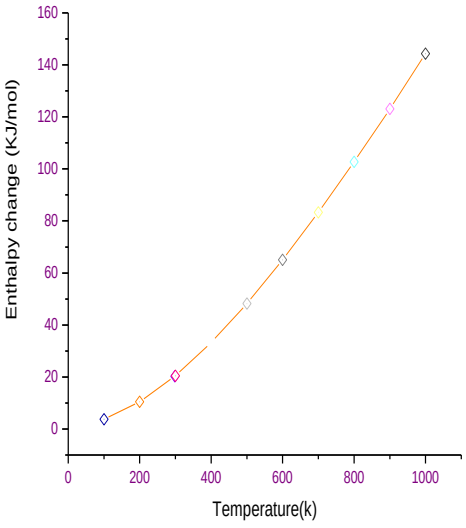

Fig 7. The effect of temperature on enthalpy change (ΔH0→T) of 3,5-diamino-1,2,4-triazole

Table 9. Thermodynamic properties of 3,5-diamino-1,2,4-triazole determined at different temperatures with B3LYP/6-311+G(d,p) level

T (K)	S (J/mol.K)	Cp (J/mol.K)	ΔH0→T (kJ/mol)
100	247.69	49.09	3.74
200.00	292.91	84.75	10.47
298.15	332.38	114.01	20.26
300.00	333.08	114.51	20.47
400.00	369.54	139.38	33.21
500.00	402.91	159.68	48.20
600.00	433.51	175.92	65.01
700.00	461.64	188.95	83.27
800.00	487.59	199.60	102.72
900.00	511.63	208.52	123.14
1000.00	534.01	216.13	144.38

Vibrational Spectra

The molecular structure of DAT belongs to C_1 point group symmetry. For C_1 symmetry there would not be any relevant distribution. The molecule consists of 12 atoms and expected to have 30 normal modes of vibrations of the same species (A) under C_1 symmetry. The harmonic vibrational frequencies calculated for DAT at B3LYP level using the triple split valence basis set along with the diffuse and polarization functions, 6-311+G(d,p) basis set. The maximum number of potentially active observable fundamentals of a non-linear compound that contains N atoms is equal to (3N-6). Accurate vibrational frequency assignment for aromatic and other conjugated system is necessary for characterization of compound. For visual comparison, the observed and calculated FTIR and FT-Raman spectra of DAT at HF and DFT/B3LYP level using 6-311+G(d,p) basis set are shown in Figs. 8 and 9, respectively.

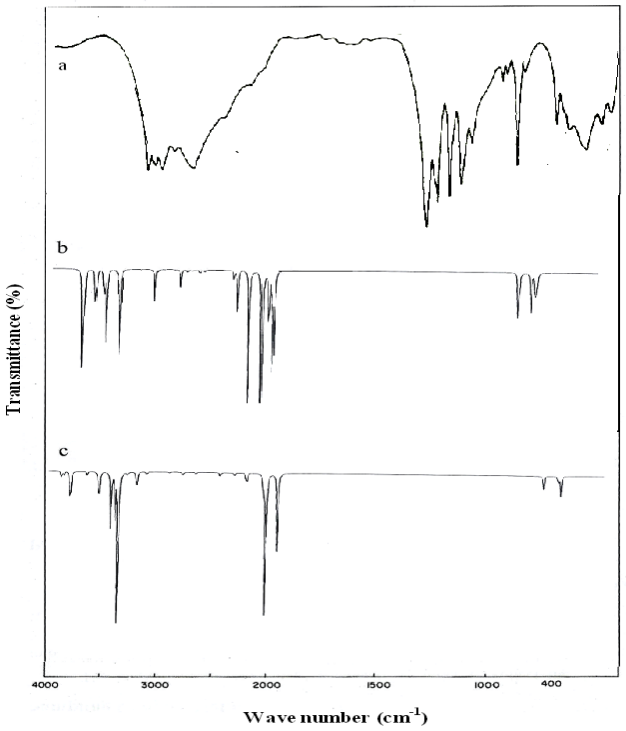

Fig 8. Comparison of observed and calculated IR spectra of 3,5-diamino-1,2,4-triazole (a) observed in solid phase, (b) calculated with B3LYP\6-311+G(d,p) and calculated with HF\6-311+G(d,p)

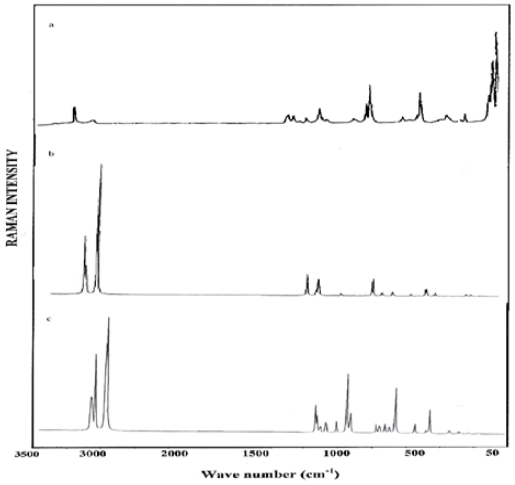

Fig 9. Comparison of observed and calculated Raman spectra of 3,5-diamino-1,2,4-triazole (a) observed in solid phase, (b) calculated with B3LYP\6-311+G(d,p) and calculated with HF\6-311+G(d,p)

The detailed vibrational assignment of fundamental modes of DAT along with the calculated IR and Raman frequencies and normal mode descriptions (characterize by TED) are reported in Table 10.

Table 10. The charge distribution calculated by the Mulliken atomic chargesmethod for 3,5-diamino-1,2,4-triazole DFT/6-311+(d,p) basis set

Atoms	B3LYP/6-311+G(d,p)
N1	-0.318240
N2	-0.222823
C3	0.485407
N4	-0.685051
C5	0.585277
N6	-0.699772
H7	0.287984
H8	0.325680
N9	-0.739649
H10	0.309225
H11	0.324728
H12	0.347235

Comparison of frequencies calculated at HF and B3LYP with experimental values reveal the overestimation of the calculated vibrational modes due to neglect of harmonicity in real system. Inclusion of electrons correlation in DFT values smaller in comparison with the HF frequencies data. The calculated frequencies are slightly higher than the observed value for the majority of normal modes. The major factor which is responsible for these discrepancies between the experimental and computed value is related to the fact that the experimental value is an anharmonic frequency while the calculated value is harmonic frequency. While anharmonicity is the main factor of the discrepancies in the case of vibrations related to the NH_2 bond, for other vibrations most of the discrepancies come from the approximate nature of the used computational technique, and probably also from the lattice effects in the substance. The comparative graph of calculated vibrational frequencies by HF and DFT methods at HF/6-311+G(d,p), and B3LYP/6-311+G(d,p) basis sets for the DAT are given in Fig. 10.

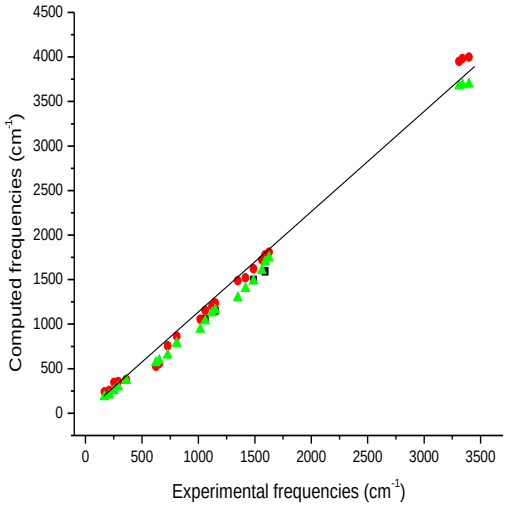

Fig 10. Comparative graph of computed frequencies (HF and DFT) with experimental frequencies

From the figure ,it is found that the calculated (unscaled) frequencies by B3LYP with 6-311+G(d,p) basis sets are closer to the experimental frequencies than HF method with 6-311+G(d,p) basis set. This observation is supported by the literature report.

N-H vibrations

It has been observed that the presence of N–H in various molecules may be correlated with a constant occurrence of absorption bands whose positions are slightly altered from one compound

to another, this is because the atomic group vibrates independently of the other groups in the molecule and has its own frequency. In all the heterocyclic compounds, the N–H stretching vibrations occur in the region 3500–3000cm−1. The position of absorption in this region depends upon the degree of hydrogen bonding, and hence upon the physical state of the sample. The spectral lines assigned to N–H stretching vibrations have shifted to higher region in the present system. It clearly indicates that the stretching of N–H bond upon protonation has shifted the frequency to a higher region. Another possible cause for the stretching may be due to the occurrence of N–H and C–H hydrogen bonds in the atomic sites of the pyrimidine and imidazole rings. Hence, in the present investigation, the N–H stretching vibrations have been found at 3095cm−1 in IR and 3096cm−1 in Raman, which are further supported by the PED contribution of almost 100%. The in-plane and out-of-plane bending vibrations of N–H group are also supported by the literature [37].

NH_2 Vibrations

The DAT molecule under consideration posses NH_2 group and hence six internal modes of vibration are possible such as symmetric stretching, asymmetric stretching, scissoring, rocking, wagging and torsional mode. The frequency of asymmetric vibration is higher than that of symmetric one. The frequencies of amino group in the region 3500 - 3300 cm^{-1} for NH stretching, 1700 - 1600 cm^{-1} for scissoring and 1150 - 900 cm^{-1} for rocking deformation. In the present investigation, the asymmetric and symmetric modes of NH_2 group are assigned at 3398, 3340 and 3310 cm^{-1} for FTIR and 3237 cm^{-1} for Raman bands, respectively. The band observed at 1616 and 1631cm^{-1} for FTIR and Raman spectrum is assigned to NH_2 scissoring mode. The rocking, wagging, twisting deformation vibrations of NH_2 contribute to several normal modes in the low frequency region. The band observed at 808 cm^{-1} for FTIR and 795 cm^{-1} in Raman is assigned to NH_2 rocking vibrations and the FT-IR and Raman band observed at 653 cm^{-1} and 665 cm^{-1} is assigned to NH_2 wagging modes, and the band observed at 212 and 168 cm^{-1} in FTIR is assigned to NH_2 twisting modes [37].

C-N Vibrations

In aromatic compounds, the C–N stretching vibration usually lies in the region 1400–1200cm−1. The identification of C–N stretching frequencies is a rather difficult task. Since the mixing of

vibrations is possible in this region [29,37]. In this study, the bands observed at 1462,1441,1432,1350 in IR and 1489,1463,1433cm−1 in Raman spectrum have been assigned to C–N stretching vibration of DAT. The in-plane and out-of-plane bending C–N vibrations have also been identified and presented in Table 11 for the title compound. These assignments are also supported by the TED values.

Mulliken

The very small variations in bond lengths and angles relative to the unsubstituted compound, suggests little significant interaction of the 3,5-amino groups with the 1,2,4-triazole ring. The electron distributions should show the same effect. The Mulliken analyses of these three molecules (Table 10) show that the amino group is indeed almost electrically neutral overall, although highly polarized $N^{\delta-}$–$H^{\delta+}$ within the group. Since C–H is polarized $C^{\delta-}$–$H^{\delta+}$, replacement of H by NH2 reduces the total density on the ring atoms. However, there is additional density at both N-atoms at the expense of the central C in the associated NCN units; thus in the 3-amino compound, C3 looses density to N in the N2–C3–N4 unit; similarly, in the 5-amino compound, C5 looses density to N1 and N4. Thus some polarization does occur when the amino group is present. In all three compounds, N1 and N4 have higher atomic population than do the N2 atoms. We have previously shown that the Mulliken population analyses, and the derived net atomic charges, can be converted into a set of bond dipoles, by summing charges about the atomic centre's [38], and solving a series of simultaneous equations for the individual bond moments. The understanding of the changes is based upon the observation that these populations show a strong donation in all cases from H to attached C (0.16e) or N (0.27e). For the un substituted 1,2,4-triazole ring this shows that N1 is a strong donor (0.1e) towards N2, while C3 is a weak donor to N4; N1 is a very weak donor to C5, which is a strong donor (0.13e) to N4. The principal effect of the 3-amino group (which is almost electrically neutral in itself) relative to a 3H-atom, is to change the sign of C3 to negative, and hence to donate electrons to both N2 and N4, which reverses the N2 to C3 donation in the parent compound. Similarly, the 5-amino group (which is again nearly electrically neutral) by replacing the 5-H (a strong donor) reverses the charge on C5 which becomes positive (0.2e) but donates to the neighbour atoms N1 and N4. The 3-amino group is not electrically neutral, being a donor to N1 by ~0.07e; however, again the replacement of 1H by amino, leads to N1 becoming positive, otherwise the effect of the amino substituent is very small. The effects of very small bond polarizations (charge migrations) can be seen in these procedures (Fig. 11), even including the effect of the unsymmetrical orientation of the amino group in the 5-amino-1,2,4-triazole.

Table 11. The observed FTIR , FT-Raman and calculated (unscaled and scaled) frequencies(cm^{-1}), IR intensity (km mol^{-1}),Raman activity (A^0 amu-1) and force constant (m dyne A^0) and probable assignments(Characterized by TED) of 3,5-diamino-1,2,4-triazole using HF/6-31+G(d,p) and B3LYP /6-31+G(d,p) calculations.

Symmetry species C_1	Observed frequencies (cm^{-1})		Calculated frequencies(cm^{-1}) (Unscaled)		Scaling frequency (cm^{-1})		Force constant (mDyne/A)		IR intensity (KM/Mole)		Raman activity (A^4/amu)		Assignment (% TED)
	FTIR	FT-Raman	HF	B3LYP	HF	B3LYP	HF	B3LYP	HF	B3LYP	HF	B3LYP	
A	3398s	--	3999	3695	4395	3396	10.421	8.8490	80.217	27.972	65.7803	43.7251	NH_2ass(99)
A	3340vs	--	3982	3686	4350	3342	10.335	8.8492	116.04	23.917	65.5454	102.121	NH_2ass(99)
A	3310ms	--	3949	3674	4308	3313	9.9733	8.637	136.00	28.297	124.312	100.947	NH_2ss(98)
A	--	3237w	3856	3574	4215	3235	9.1724	7.8769	87.993	1.0675	160.673	317.923	NH_2ss(97)
A	3095s	3096w	3844	3456	4082	3094	8.1123	5.5678	120.66	31.543	132.342	50.0854	νNH(80), NH_2ss(18)
A	--	1631vw	3824	3411	4014	1633	9.1185	7.8751	127.98	38.575	143.495	55.0861	NH_2siss(93), νCN(3)
A	1616vs	--	2825	2769	2333	1617	2.8590	2.0062	254.38	7.4250	23.8326	32.8114	NH_2siss(91), νCN(5)
A	--	1489ms	2808	2745	2220	1486	2.6628	1.9419	272.41	201.44	12.1261	4.3941	νCN(88) ,NH_2siss(11
A	1462s	1463ms	2777	2698	2201	1460	3.8005	6.1469	273.32	365.39	8.9468	5.6459	νCN(93),νNH(6)
A	1441s	--	2722	2604	2133	1444	7.4880	9.4039	699.24	61.884	13.8304	41.3787	νCN(92), bRing1(8)
A	1432vs	1433ms	2621	2484	2089	1430	8.8189	6.3253	420.43	42.443	9.0460	0.5390	νCN(91), bRing2(4)
A	1418s	--	2519	2398	2019	1419	3.0982	4.9787	126.21	7.3236	46.1167	3.5866	νCN(90) bNH(5)
A	1350vs	--	2487	2297	2007	1353	3.0094	1.5400	35.331	13.011	18.3937	0.2271	νCN(82), NH_2rock(12)
A	1122s	--	2201	2124	1999	1124	3.5115	1.3371	20.840	1.8422	9.6317	2.4378	νNN(80), νCN(15)
A	1061ms	1057ms	2153	2037	1989	1064	1.6128	2.0344	4.3462	8.4884	7.0736	6.6848	bRing1(77), NH_2rock(15)
A	--	1028s	2110	2019	1967	1628	1.9398	2.4469	15.481	0.3849	7.8380	0.6121	bRing2(76), ωNH(14)
A	1017ms	--	2054	1942	1920	1019	2.8586	4.7248	56.035	3.4923	33.6619	6.7125	bNH(75), NH_2wag(15)
A	808w	--	1865	1785	1879	812	2.9600	1.9893	6.8471	6.4456	6.4569	3.6721	NH_2rock(84) ,NH_2wag(8)
A	--	795ms	1837	1716	1223	797	4.6623	2.2445	88.669	55.920	0.4430	0.7742	NH_2rock(83), τRing1(5)
A	728ms	--	1756	1652	1100	729	3.0283	1.5453	0.0541	3.0845	1.7992	13.6529	ωNH(82), τRing2(7)
A	--	665w	1721	1647	1009	667	1.7520	2.4309	12.670	3.6757	15.427	0.5414	NH_2wag(81) bCN(8)
A	653vs	--	1655	1591	978	655	0.2110	0.2696	333.36	389.00	0.4990	1.1894	NH_2wag(79) bCN(11)
A	624s	--	1527	1567	988	626	0.4609	0.2723	4.9979	117.73	3.7008	4.2250	τRing 1(80) ωCN(9)
A	--	468vw	1442	1536	951	469	0.1393	0.2302	244.80	144.36	1.5869	0.6295	τRing 2(78) ωCN(10)
A	--	377vw	1419	1452	879	379	0.1217	0.2770	107.85	111.29	0.5565	1.0416	bCN(77) NH_2twist(11)
A	361s	--	1377	1367	855	365	0.3224	0.3151	0.9196	10.191	0.1387	0.1749	bCN(76)
A	290ms	--	1354	1294	693	293	0.0829	0.1656	146.23	0.0406	0.5367	2.8917	ωCN(75)
A	254s	--	1345	1251	657	257	0.2050	0.0385	18.944	117.91	1.0138	3.7430	ωCN(69)
A	212w	--	1256	1205	515	215	0.0794	0.0786	242.79	11.367	0.8724	0.0648	NH_2twist(65)
A	168vw	--	1240	1186	469	169	0.0588	0.0230	335.04	18.777	0.2664	1.0717	NH_2twist(59)

Abbreviations

ν - stretching; b - in-plane bending; ω - out-of-plane bending; asymd - asymmetric; symd - symmetric; t - torsion; trig - trigonal; w - weak; vw-very week; vs - very strong; s - strong; ms - medium strong; ss - symmetric stretching; ass - asymmetric stretching; ips - in-plane stretching,; ops - out-of-plane stretching; sb - symmetric bending; ipr - in-plane rocking; opr - out-of-plane rocking; opb - out-of-plane bending.

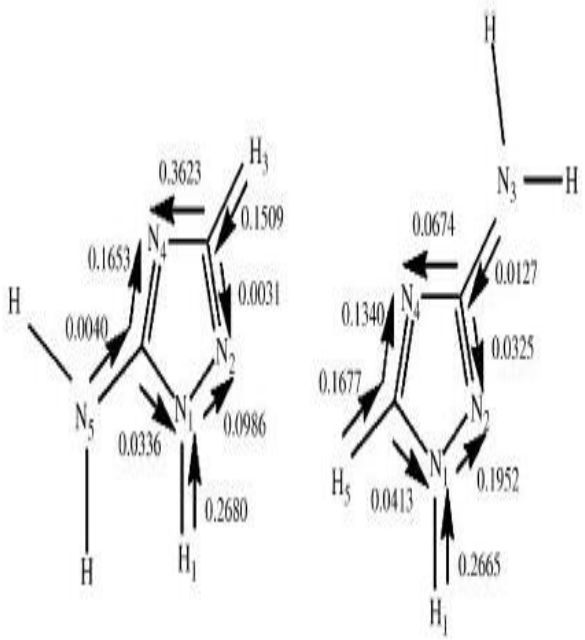

Fig 11. Bond dipoles derived from the atomic populations by Mulliken method

The electric field gradients and derived ^{14}N nuclear quadrupole coupling constants for the 1H-series of unsubstituted, and 3- and 5-amino-1,2,4-triazoles

In this section we adopt the NQR convention for magnitudes, namely $|qzz| \geq |qyy| \geq |qxx|$, and we use our previous other convention to define directions for EFG tensor elements in these ring systems. A EFG element which is close to internally bisecting the ring angle, and hence passes close to the ring centre, is radial (R), the other in-plane element is close to tangential at the ring atom (T), while the out-of-plane component is locally the p-direction. Even though distortion of these positions occurs when differing atoms lie at adjacent positions, these terms are still applicable, as seen in Figs. 12–14. And charge distribution on the molecule has an important influence on the vibrational spectra. The corresponding Mulliken's plot is shown in Figure. 15.

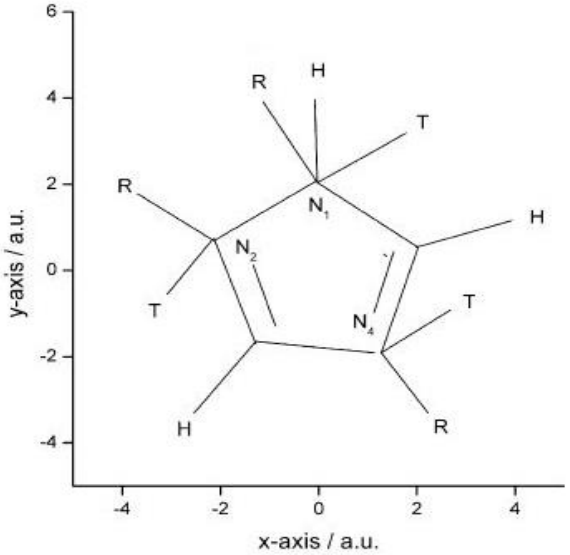

Fig 12. The electric field gradients for 1H-1,2,4-triazole. Mulliken method.

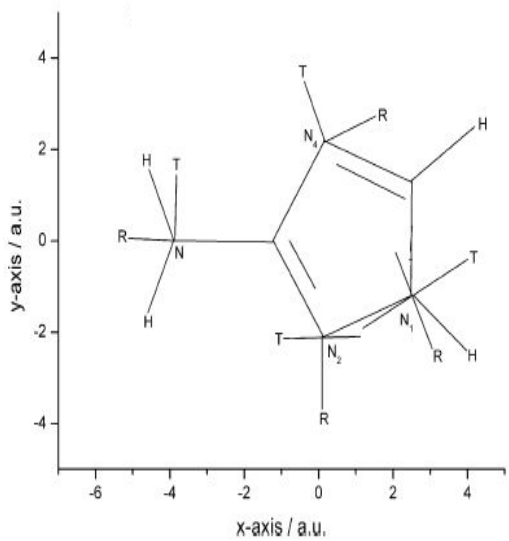

Fig 13. The electric field gradients for 3 amino-1,2,4-triazole by Mulliken method.

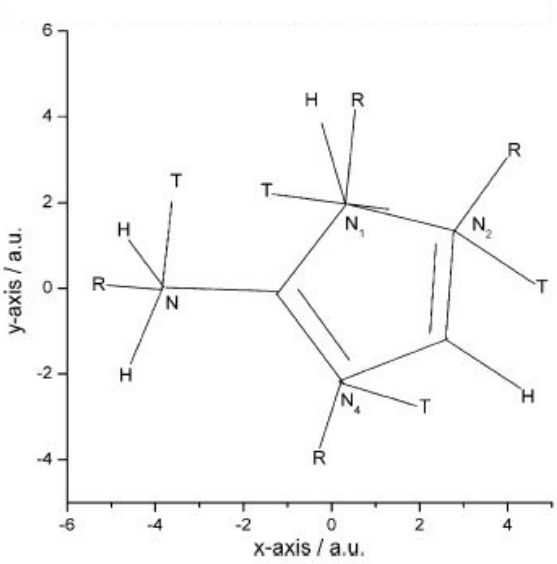

Fig 14.The electric field gradients for 5 amino-1,2,4-triazole by Mulliken method

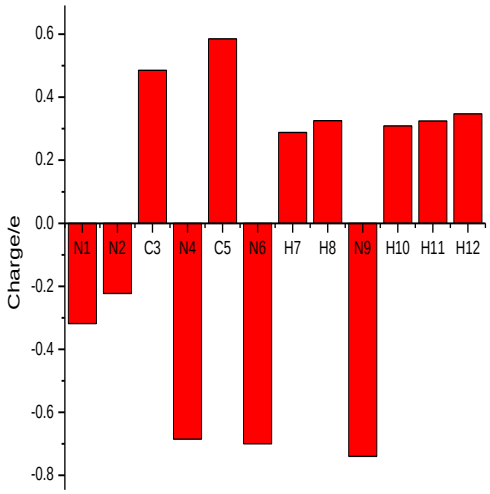

Fig 15. Mulliken plot of 3,5-diamino-1,2,4-triazole.

Conclusion

Molecular structure, FT-IR, FT-Raman, UV and quantum chemical calculation studies have been performed on 3,5-diamino-1,2,4-triazole in order to identify its structural and

spectroscopic features. The title compound was theoretically optimized using *ab initio* HF and DFT (B3LYP/6-311+ G (d,p)) and the optimized geometry are tabulated in comparison with the experimental

data and well discussed. The complete vibrational assignment with TED was calculated. Molecular orbital coefficient analysis suggests that the electronic spectrum corresponds to the $\pi-\pi^*$ electronic transaction. The Non-Linear Optical (NLO) properties were calculated theoretically the predicated first hyperpolarizability values 12 times greater than those of urea. These sites give information about the region from where the compound can undergo non-covalent interaction. HOMO, LUMO, Mulliken and NMR chemical shifts was calculated and compared with the experimental data. Finally, the thermodynamic properties to the title compound have been calculated for different temperatures, revealing the correlations among ((Cp), (S) and ($\Delta H0\rightarrow T$)) and temperatures are obtained.

References

[1] O. Kahn, C.J. Martinez, Science 279 (1998) 44.

[2] C.D. Putnam, A.S. Arvai, Y. Bourne, J.A. Tainer, J. Mol. Biol. 296 (2000) 295.

[3] E.Margoliash,A.Novogrodsky,A. Schejter, Biochem. J. 74 (1960) 339.

[4] P. Nichols, Biochim. Biophys. Acta 59 (1962) 414.

[5] H.E. Aebi, in: H.U. Bergmeyer, J. Bergmeyer, M. Gra ßl (Eds.), Methods of Enzymatic Analysis vol. 3, Verlag Chemie, Basel, 1983, p. 273.

[6] R.D. Zakharieva, A.S. Galabov, N. Nikolova, Bioorg. Med. Chem. Lett. 4 (1994) 2831.

[7] K. Fabianowska-Majewska, J.A. Duley, H.A. Simmonds, Biochem. Pharmacol. 48 (1994) 897.

[8] H. Saad, *Indian J. Chem*. 35B (1996) 980.

[9] I.B. Obot, N.O. Obi-Egbedi, S.A. Umoren, E.E. Ebenso, *Chem. Eng. Comm.* 198 (2011) 711.

[10] S. Yazici, C. Albayrak, G. Ismail, I. Senel, O. Buyukgungor, *J. Mol. Struct*. 985 (2011) 292.

[11] F. Billes, H. Endredi and G. Keresztury, *J. Mol. Struct*. *(Theochem*) 530 (2000) 183.

[12] V. K. Kumar, G. Keresztury, T. Sundius, R. J. Xavier, *Spectrochimica Acta Part A*. 61 (2005) 261.

[13] M.J. Frisch, G.W. Trucks, H.B. Schlegal, GAUSSIAN 09, Revision A.02, Gaussian, Inc., Wallingford, CT, 2009.

[14] A.D.Becke,J.Chem. Phys. 98(1993)5648-5652.

[15] C.Lee, W.Yang, R.G.Parr. Phys. Rev. B37 (1988) 785-789.

[16] P.Pulay, G. Fogarasi, G.Pongor, J.E.Boggs, A.Vargha, J. Am. chem. soc,105 (1983) 7037- 047.

[17] G. Fogarasi, P.Pulay,in: J.R.Durig(Ed.) Vibrational Spectra and Structure, Vol.14, Elsevier, Amsterdam, 1985 , P. 125, Chapter 3.

[18] T.Sundius, vib, spectrosc.29 (2002)89-95.

[19] MOLVIB (V.7.0):Calculation of Harmonic Force Fields and Vibrational Modes of Molecules, QCPE Program No. 807(2002).

[20] Chem X-B,Li K&ShiD-Q,Chinese J Struct hem 27(2008) 1389.

[21] P.L. Polavarapu, J. Phys. Chem. 94 (1990) 8106-8112.

[22] G. Keresztury, S. Holly, J. Varga, G. Besenyei, A. V. Wang, J. R. Durig, Spectrochim. Acta 49A,1993,2007.

[23] G. Keresztury, in: J. M. Chalmers, P. R. Griffiths (Eds.,), Raman spectroscopy Theory,Handbook of vibrational spectroscopy,Vol.1, John Wiley and sons Ltd.,2002,71.

[24] J. Karpagam, N. Sundaraganesan, S. Sebastain, S.Manoharan, M.Kurt, J. Raman Spectrosc, 41 (2010) 53-62.

[25] D.A.Kleinman, Phys. Rev.126 (1962) 1977-1979.

[26] http://riodbol.ibase.aist.go.jp/sdbs/(National Institute of Advanced Industrial Science).

[27] H. O. Kalinowski,S. Berger,S. Brawn,Carbon-^{13} NMR Spectroscopy. JohnWiley and Sons,Chichester,1988.

[28] K. Phhlajer,E. Kleinpeter(Eds.),Carbon-^{13} Chemical shifts in Structure and Spectrochemical analysis,VCH Publishers.Deerfield Beach,1994.

[29] Kuppusamy Sambathkumar Spectrochim. Acta A 147 (2015) 51-66.

[30] R.G..Parr, L.V.szentpaly, S.J.Liu. Am. Chem. soc. 1999, 121, 1922.

[31] P.K.Chattraj, B.Maiti, U.J.Sarkar. J. Phys. ChemA, 2003, 107, 4973.

[32] R.G.Parr, R.A.Donnelly, M.Levy, W.E.Palke. J.Am.Chem .soc. 1978, 68, 3807.

[33] R.G.Parr, R.G..Pearson, J.Am.Chem.soc.1983, 105, 7512-7516.

[34] R.G..Parr, P.K.Chattraj, J.Am.Chem.soc,1991,113,1854.

[35] R.Parthasarathi,J.Padmanabhan,B.Maiti,P.K.Chattraj,J.Phys.ChemA 2008, 107,10346, P.Thanikaivelan, V.Subramanian, J.RaghavRao, B.V.Nair, Chem. Phys.Let 2000,323,59.R.Parthasathi; J.Padmanabhan, M.Elango, V.Subramanian, K.Chattraj,Chem.Phys.Lett. 2004,394,225.

[36] R.Parthasarathi, J.Padmanabhan, V.Subramanian, B.Maiti, P.K.Chattraj, Curr. Sci.2004, 86,535.

[37] K. Sambathkumar ,S. Jeyavijayan ,M. Arivazhagan Spectrochim. Acta A 147 (2015) 124-138.

[38] H. Palmer, Dines Christen J. Mol. Struct 705 (2004) 177–187.

[39] http://riodbol.ibase.aist.go.jp/sdbs/(National Institute of Advanced Industrial Science).